Available online at www.sciencedirect.com
SCIENCE DIRECT
Journal of Photochemistry and Photobiology A: Chemistry 177 (2006) 197–204
Journal of Photochemistry and Photobiology A:Chemistry
www.elsevier.com/locate/jphotochem

Edge excitation red shift and energy migration in quinine bisulphate dication

H. Mishra *, Debi Pant [1], T.C. Pant, H.B. Tripathi

Photophysics Laboratory, Department of Physics, Kumaun University, Nainital-263001, India

Received 28 June 2004; received in revised form 21 March 2005; accepted 30 May 2005
Available online 11 July 2005

Abstract

Photoinduced excited state dynamical processes in quinine sulphate dication (QSD) have been studied over a wide range of solute concentrations using steady state and nanosecond time-resolved fluorescence spectroscopic techniques. The edge excitation red shift (EERS) of emission maximum, emission wavelength dependence of fluorescence lifetimes and the time dependence of emission maximum are known to occur due to the solvent relaxation process. With increase in solute concentration, the emission spectrum shifts towards the lower frequencies accompanied with decrease in fluorescence intensity, however, absorption spectrum remains unchanged. A decrease in EERS, fluorescence lifetimes, time dependent fluorescence Stokes shift (TDFSS), fluorescence polarization and the solvent relaxation time (τ_r) is observed with the increase in solute concentration. The process of energy migration among the QSD ions along with solvent relaxation has been found responsible for the above experimental findings.

Keywords: Quinine sulphate dication; EERS; Energy migration

1. Introduction

The photophysics of quinine sulfate dication (QSD) (Quinine sulphate in 0.1N H_2SO_4 solution of water) has been the subject of extensive research in the past because of its medical applications as well as its use as a fluorescence standard [1–5]. The quantum yield of the QSD (10^{-5} M) measured by Melhuish [1] long back ($\phi_f = 0.56$) is still in use today. However, it was demonstrated [2,6] that excitation spectrum of QSD was different from its absorption spectrum. Chen [7] found red shift in emission spectrum of QSD on excitation at red edge of absorption band (REE effect) and suggested that it arises due to two close lying states, but Fletcher [8] interpreted this effect as being due to the molecules existing in at least two different conformers each with its own electronic transition based on solvent relaxation modes. It is generally found that solvent bonding to chromophore restricts the position of auxochrome, which exists at least in two average conformers. The excitation dependence of the emission of polar aromatic molecules in viscous polar solvents is a common feature [9] and is in general related to microenviromental heterogeneity. Ioth and Azumi [10] gave an explanation that on excitation at the red edge of the absorption band only certain configurations are excited, resulting into red shifted emission which lacks some high frequency components compared to that due to short wavelength excitation.

QSD is one of the rare emitters in which excited state solvent relaxation appears to occur on nano-second time scale even at ambient temperature [16]. Thus, time-resolved emission spectroscopy (TRES) and other dynamical studies, which depend on solvent relaxation, could easily be measured using QSD as an emitter. Like several other solvent probe molecules, QSD is highly sensitive to the surrounding solvent environment and undergoes a large change of dipole moment upon electronic excitation, yet it could not be used as an ideal probe molecule for the quantitative studies of the

* Corresponding author. Tel.: +91 5942 237450; fax: +91 5942 235576.
E-mail addresses: hirdyesh@yahoo.com (H. Mishra), debidatta_pant@schi.scf.ch (D. Pant), tc_pant@yahoo.com (T.C. Pant), herabtripathi@yahoo.com (H.B. Tripathi).
[1] Present address: Laboratoire d'Electrochimie, Ecole Polytechnique Fédérale de Lausanne, CH-1015 Lausanne, Switzerland.

1010-6030/$ – see front matter © 2005 Elsevier B.V. All rights reserved.
doi:10.1016/j.jphotochem.2005.05.026

solvation process because of its complex decay kinetics. The fluorescence decay has been found to exhibit a bi-exponential decay at the shorter wavelength edge and a rise in decay is observed at the red edge of the emission band [11–14]. The non-exponential nature of the fluorescence decay has been attributed to the solvent relaxation process. The photophysics of quinine sulfate and related compounds in different solvents and at various temperatures has been reported from this laboratory [15–20]. It was shown that the methoxy group plays an important role in the photophysics of these molecules. From the temperature dependence of fluorescence characteristics, it was suggested that around 160 K a rapid charge transfer from methoxy group to the quinoline ring take place, followed by solvent relaxation at ambient temperature in the polar fluid medium [16]. Thus, these processes lead to change in the charge density distribution and geometry of the fluorophore, which combined with solvent relaxation, give a multi exponential decay.

The photophysical processes in QSD and related molecules have been explored for designing fluorescence optical sensors for halides [21,22] and as a probe for measuring free volume in membrane or sol–gel glasses [23]. We have also shown that the magnitude of EERS in QSD can be used as a probe to determine the micro-environmental nature of the polymers [24]. Despite the widespread interest and importance of QSD, its photophysical properties as a function of solute concentration has not been studied in detail. In this paper we report anomalies in spectral properties and fluorescence decay parameters of QSD in fluid media for its different concentrations. The process of energy migration along with solvent relaxation have been found responsible for the observed dynamical behavior at the higher concentrations of QSD.

2. Experimental

2.1. Material

Quinine bisulphate (QS) from Aldrich was re-crystallized from water. All the solvents were either of spectroscopic grades or were checked for their purity. All the samples of QSD were prepared by dissolving the appropriate concentration of QS in 1N H_2SO_4 containing HPLC grade water (SRL SISCO laboratory chemicals).

2.2. Steady state measurements

Absorption spectra were taken with the help of dual beam JASCO V-550 spectrophotometer and fluorescence and excitation spectra were recorded with the help of JASCO FP-777 [25] spectrofluorometer and JOBIN-YVON-SPEX fluorolog having double monochromator in both excitation and emission path. The data were analyzed using related software GRAMS/32. Polarization measurements were carried out with the help of Spex fluorolog with polarization accessories. The fluorescence intensity component (I_{vv}, I_{vh}, I_{hv} and I_{hh}), in which the subscripts refer to horizontal (h) and vertical (v) positioning of the excitation and emission polarizer respectively, were used to calculate the steady state fluorescence polarization using following equation:

$$P = \frac{I_{vv} - GI_{vh}}{I_{vv} + GI_{vh}} \quad (1)$$

where G is the grating correction factor and is equal to I_{hv}/I_{hh}. In all cases the background intensity of the reference was subtracted from the sample emission spectra to eliminate the errors due to scattering artifacts. All experiments were done with multiple set of samples for each concentration and thus the polarization curve is an average of different data sets. The spectral shifts obtained with different sets of samples were identical in most of the cases and values were with in ± 1.0 nm.

2.3. Time domain measurements

Fluorescence decay times and time-resolved emission spectra were recorded with the help of Edinburgh 199 time domain spectrometer and analyzed by software FLA-199 in PHA and MCA mode. The excitation source was a thyratron gated nanosecond flash lamp with hydrogen as the filler gas. Lamp profile where measured at the excitation wavelength using Ludox scatterer. The pulse width was about 1.0 ns with repetition rate of 20 kHz. The decay times were determined using non-linear least square method by time correlated single photon counting (TCSPC) technique. Care was taken in data analysis to differentiate between the mono-exponential and bi-exponential fits by judging the χ^2 values standard deviations and weighted residuals. Intensity decay curves so obtained were fitted to sum of exponential terms as

$$I(\tau, t) = \alpha_1 \exp^{-t/\tau_1} \pm \alpha_2 \exp^{-t/\tau_2} \quad (2)$$

where τ_1, τ_2 are the shorter and longer lifetime components, respectively, and α_1, α_2 are the corresponding amplitudes in QSD [16]. The negative sign indicate the rise time at the red edge of the emission of the QSD. The average decay time $\langle\tau\rangle$ for bi-exponential decays of fluorescence were calculated from the observed decay times (τ_1, τ_2) and pre-exponential factors (α_1, α_2) using the following equation:

$$\langle\tau\rangle = \frac{\alpha_1\tau_1 + \alpha_2\tau_2}{\alpha_1 + \alpha_2} \quad (3)$$

The time-resolved emission spectra (TRES) were also obtained with the help of FLA-199, in it the TAC is by passed, and signal from the discriminator, on the emission channel, are routed directly to the MCA/PC in single channel analyzer (SCA mode), with the channel advance rate synchronized with the wavelength drive of the emission monochromator (ORTEC timer unit 719), the resulting histogram of counts represents the fluorescence spectrum of the sample. The SCA is essentially a timing discriminator with two variable levels V_L and V_U. Input pulses having amplitude lower than V_L and

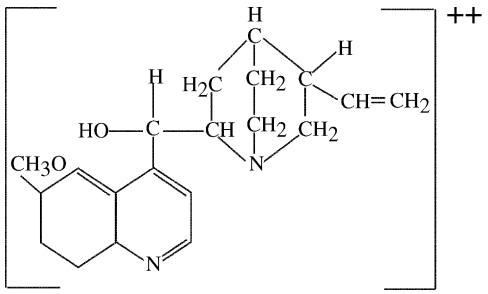

Fig. 1. Structure of QSD.

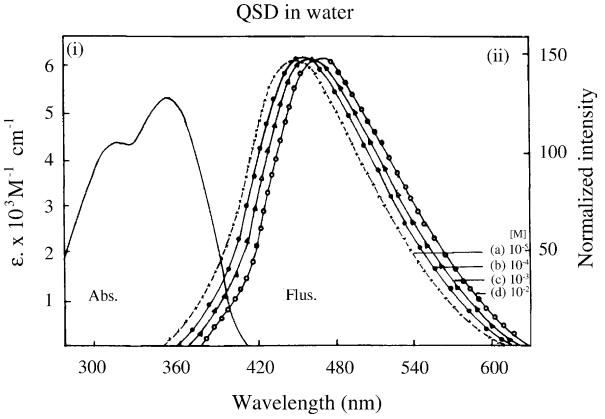

Fig. 2. (i) Absorption spectrum of QSD in water (1N H_2SO_4) at 20 °C in 10^{-5} M. (ii) Normalized emission spectra of QSD in water (1N H_2SO_4) excited by 360 nm for different concentrations.

higher than V_U are rejected. Spectra recorded by the above method, after a certain time delay Δt, within a time window δt, selected by upper level discriminator (ULD) and lower level discriminator (LLD). Photon in discrete time intervals are summed and arranged as a function of wavelengths.

3. Results and discussion

In dilute sulphuric acid solutions (0.1N H_2SO_4), quinine sulphate is present as a di-cationic species, which is quite stable [16]. The molecular structure of QSD is shown in Fig. 1.

The absorption and the emission spectra of QSD for different concentrations of solute are shown in Fig. 2. The absorption spectrum shows two bands L_a and L_b at 346 and 316 nm, respectively (Fig. 2i), whereas, the emission spectrum has only a structure-less broadband for all the concentrations studied. It is also observed that the position of absorption bands and the corresponding molar absorption coefficient (ε) values do not change with concentration of the solute molecule, which rules out any possibility of dimer formation. However, the emission spectrum (Fig. 2ii) shifts towards the lower frequencies with the increase in solute concentration. The full width at half maximum (FWHM) of the emission spectrum also decreases with the solute concentration. It is observed that the excitation spectrum of QSD fails to coincide with the red edge of the absorption band and the quantum yield increases when monitored at different increasing emission wavelengths [16]. When excited at the red edge of the first absorption band the emission maximum shifts towards the lower frequency side for all the concentrations of solute studied. This shift in emission spectrum on excitation at the red edge of the absorption spectrum is known as edge excitation red shift (EERS) as shown in the normalized emission spectra of QSD in water for concentrations (i) 10^{-2} M and (ii) 10^{-5} M in Fig. 3. The magnitude of EERS expressed as the difference in wave number (cm^{-1}) between the emission maximum obtained on 360 nm excitation and 420 nm excitation, decreases with the increase of the solute concentration. The EERS and FWHM values as obtained for different concentration of QSD are given in Table 1.

The decay fits to a bi-exponential function for all the concentrations of QSD studied. The bi-exponential fit gives the

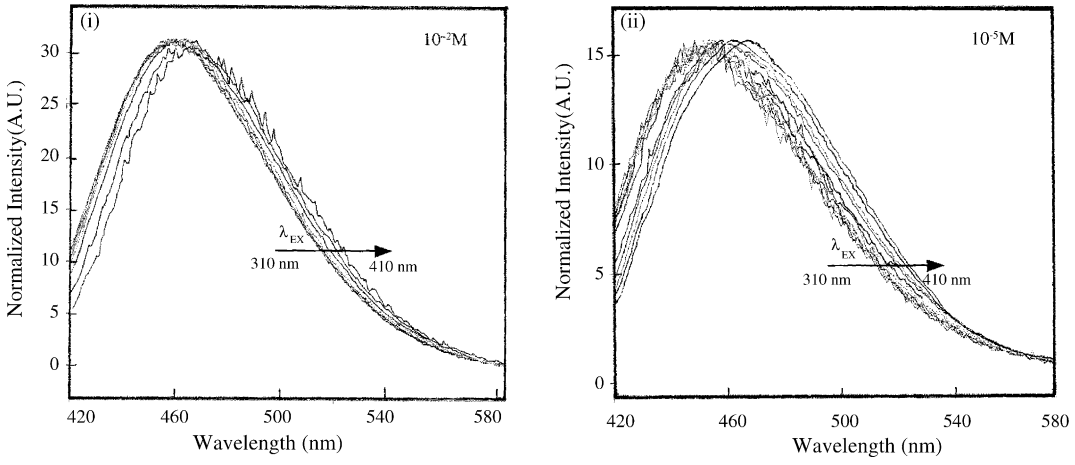

Fig. 3. Normalized emission spectra of QS in water (1N H_2SO_4) excited by different wavelengths from 310 to 410 nm for concentrations (i) 10^{-2} M and (ii) 10^{-5} M.

Table 1
Fluorescence parameters of QSD for different concentrations in water (in 1N H_2SO_4)

Concentration [M]	τ_1 (ns)	τ_2 (ns)	χ^2	α_1	α_2	τ_r (ns)	$\langle\tau\rangle$ (ns)	ϕ	FWHM (cm^{-1})	EERS (cm^{-1})
10^{-5}	2.75 (0.12)	19.43 (0.05)	1.04	0.041	0.091	6.5	14.24	0.55	4550	840
10^{-4}	2.80 (0.14)	19.36 (0.05)	1.01	0.042	0.094	6.3	14.24	0.55	4350	740
10^{-3}	2.60 (0.13)	17.50 (0.05)	1.05	0.043	0.082	5.5	12.37	0.47	4241	550
10^{-2}	2.10 (0.09)	15.70 (0.04)	1.04	0.075	0.102	5.1	9.93	0.38	4190	500
5×10^{-2}	1.60 (0.07)	12.90 (0.04)	1.16	0.099	0.093	4.7	7.07	0.27	4120	452
10^{-1}	1.60 (0.1)	8.10 (0.03)	1.21	0.093	0.099	–	4.95	0.19	4080	375

Decay measured by λ_{ex} = 360 nm at λ_{em} = 390 nm (standard deviations are given in the parentheses and τ_{rad} = 25.89 ns).

negative amplitude corresponding to the τ_1 decay component at the red edge of the emission spectrum (above 500 nm) for all the concentration studied and τ_2 continuously increases with the increase in emission wavelength. The major change in magnitude of τ_2 occurs between 390 and 450 nm while at longer emission wavelengths (500–575 nm), the increase is small. The contribution of the τ_1 component to total fluorescence intensity at blue edge is about 7% and at the red edge is only 2% whereas the long lived component τ_2 dominates throughout the emission band [16]. However, with the increase in solute concentration both the lifetime components decrease as shown in Table 1 and Fig. 4 for (i) 10^{-2} M and (ii) 10^{-5} M solutions.

The fluorescence quantum yield (ϕ) for various concentrations of QSD has been calculated with the help of following equation [26]:

$$\phi = \left[\frac{\alpha_1\tau_1 + \alpha_2\tau_2}{\alpha_1 + \alpha_2}\right]\tau_{rad.}^{-1} \quad (4)$$

where $\tau_{rad.}$ is the calculated radiative decay time and has been calculated from well known Stickler and Berg [27] relationship; from the absorption and emission spectra and extension coefficient for 10^{-5} M aqueous solution of QSD. It comes out 25.89 ns. This has value 0.55, for 10^{-5} M solution and is in agreement with the values reported by Demas and Crosby [28]. Clearly, the value of ϕ (Table 1) decreases with the increase in solute concentration.

In time-resolved spectral measurements, a time dependent fluorescence Stokes shift (TDFSS) is observed for all the concentrations studied. Fig. 5 shows peak normalized time-

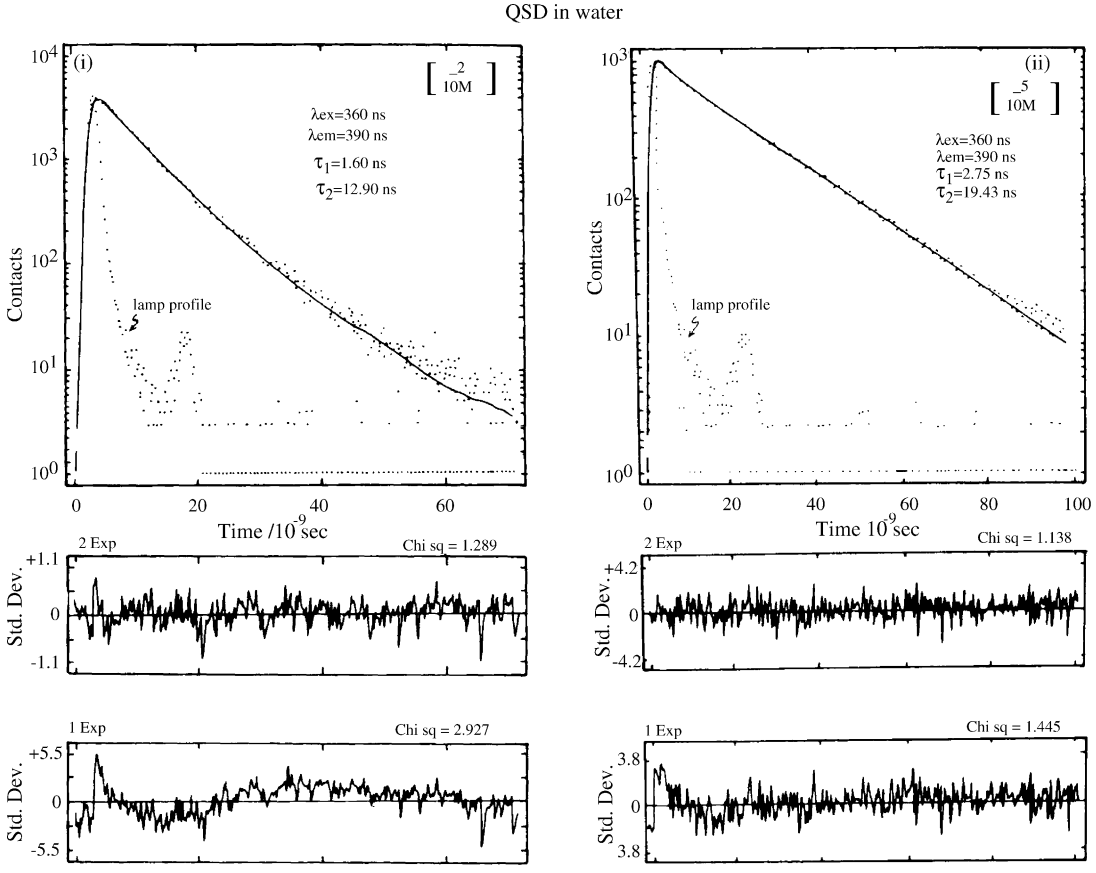

Fig. 4. Decay curves of QSD in water at (i) 10^{-2} M and (ii) 10^{-5} M concentrations, λ_{Ex} = 360 nm and emission monitored at λ_{em} = 390 nm.

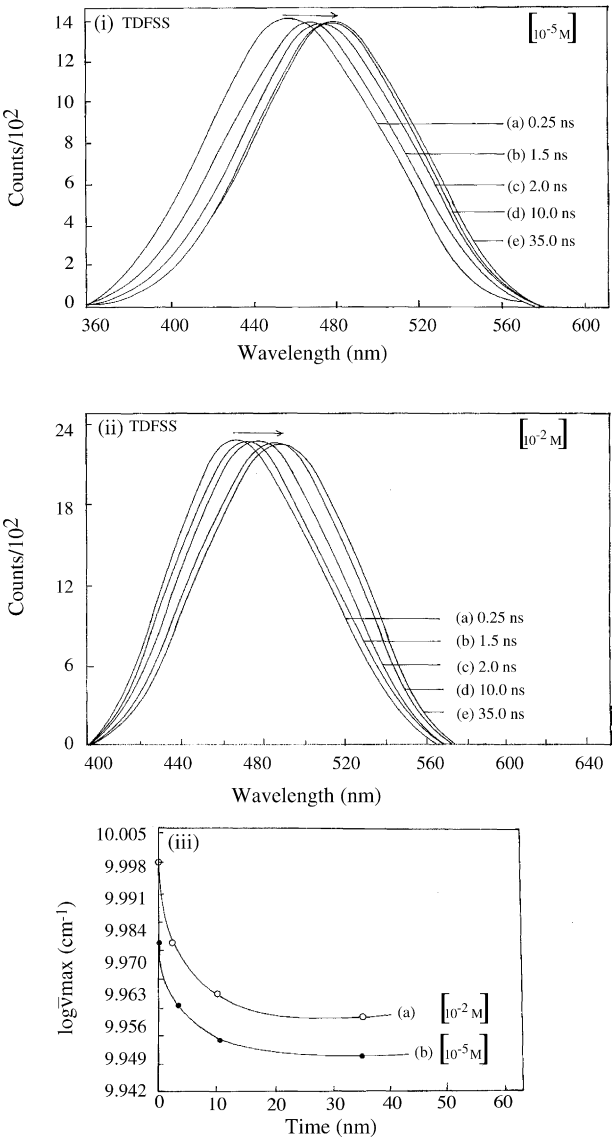

Fig. 5. Normalized TDFSS of QSD in water (1N H_2SO_4) at 20 °C in (i) 10^{-5} M and (ii) 10^{-2} M at (a) 0.25 ns, (b) 1 ns, (c) 2 ns, (d) 10 ns, (e) 35 ns. (iii) Change in the time-resolved fluorescence emission maximum of (a) 10^{-2} M and (b) 10^{-5} M QSD in water at 20 °C.

resolved emission spectra for QSD (i) 10^{-5} M and (ii) 10^{-2} M for different time windows. The time dependent change in the fluorescence emission spectrum gives a clear picture of the evolution and decay of the excited state of a fluorescent probe. It can be seen that there is a continuous red shift of the emission spectrum with increasing time window without changing its shape and FWHM. However, with increase in solute concentration the magnitude of TDFSS and FWHM decreases with the increase in solute concentration. The magnitude of the TDFSS however greater for lower concentration of QSD 900 cm^{-1} for 10^{-5} M as compared to 760 cm^{-1} for 10^{-2} M concentration. These results indicate that QSD at all concentration studied undergoes excited state solvent relaxation in nano-second time scale. The emission characteristics and complex decay kinetics of the QSD in aqueous solution could not be explained by simple two state model as one of the important features of this model is that only two lifetimes will be obtained and these values will be constant regardless of the emission wavelength. The temperature and viscosity dependence of the kinetic parameters was explained on the basis of Bakhshive's model [29] and an unusually large solvent reorientation relaxation time (7 ns) was obtained for QSD in polar fluid solvents [16]. In this model the centre of gravity of the emission is assumed to decay exponentially and shape of the emission spectrum remain constant during the emission time. While in case of two state model the half width of the emission spectrum change with times being maximum of the intermediate times [30]. No change in the shape and FWHM of the TDFSS and EERS spectra has been observed at fixed concentration although the FWHM is decreases with increase in concentration [16]. These results indicate that QCD at all concentrations studied undergoes excited state solvent relaxation in nano-second time scale. Thus the decay kinetics cannot be explained by a simple two state model of solvent relaxation rather suggest a continuous type of relaxation model. The two-state model of solvent relaxation could not explain the TDFSS, because of the observed continuous shift in TRES. However, the continuous model of solvent relaxation can be used in order to explain the broader features of complex behavior of QSD in fluid solution. The solvent relaxation time component (τ_r) values have been calculated using the continuum model and adopting the same procedure as discussed by Pant et al. [16]. According to which

$$\bar{\nu}_m(t) = \bar{\nu}_\infty + (\bar{\nu}_{0^\circ} - \bar{\nu}_\infty) \exp^{-t/\tau_r} \quad (5)$$

where $\nu_m(t)$ is the emission maximum for Gaussian shape and ν_0 and ν_∞ are the emission maxima at $t = 0$ and ∞. It is assumed that the shift to lower energy is an exponential function of solvent relaxation time τ_r as shown in Fig. 5(iii). A decrease in τ_r is observed with the increase in solute concentration.

The observation of EERS and TDFSS, increases of fluorescence lifetime with the wavelength of emission and the observation of negative amplitude for the longer wavelengths of emission are the salient features of the solvent relaxation process [9,15–20]. Generally, the relaxation of polar solvent molecules around the changed dipole moment of the excited state occurs in a pico-second time scale in fluid media and is compared with the dielectric relaxation time τ_d. However, the results presented above show that the rates of these two processes are not of the same order. The discrepancy in the values of τ_r and τ_d is due to the fact that τ_d is related to the macroscopic properties of the solvent and τ_r, responsible for EERS and TDFSS, to the microscopic environment around an excited solute molecule and hence is very likely dependent on the detailed electronic and the geometrical structures of the solute.

In our time-resolved experiments, the time resolution was not sufficient to be able to probe the ultrafast time components of water solvation. Using ultrafast time-resolved experimen-

tal techniques [31]; the solvation of water has been shown to be ultrafast with an inertial solvation time component of less than 100 fs, contributing 70% to the total solvation energy and two slower diffusive sub-picosecond time components. However, we believe the nanosecond time component we have resolved here using the dynamic Stocks shift measurements is a slowed down (due to the strong interactions of the SO_4^- ions present in the solution with the QSD molecules) diffusive time component of water solvation. There are several reports in the literature about the slower solvation time components of water in the presence of the ions in the solution. Molecular dynamics calculations and experimental data have shown slower solvation dynamics in concentrated ionic solutions than in bulk water. The interactions of water with specific cations influence the water mobility. Impey et al. [32] contrasted the interaction of water with Na^+ and K^+. Their calculations showed the residence time of water in the solvation shell around Na^+ is about twice that for water next to K^+. Their calculations also showed that residence times around divalent cations can be nanoseconds or longer. Guardia and Padro [33] calculated water interacting with Na^+ and report longer residence time of 38 ps. Wang and Tominaga [34] have used low frequency Raman spectroscopy to measure the solvent response of ionic solutions, including NaCl, KCl and $CaCl_2$ salt solutions. Their results show that the ions in solution cause relaxation times to become progressively longer with increasing concentration. Obst and Bradaczek [35] found that the interaction of Ca^{2+} ions was significantly stronger than the interaction of alkali ions with water. Using a combined quantum mechanical/molecular mechanical dynamics calculation, Tongraar et al. [36] have shown that the translational, librational and vibrational motion of water near Ca^{2+} is perturbed due to ion water interactions.

On shorter wavelengths of excitation (SWE), the emission maximum shifts towards the lower frequencies with the increase in concentration. However, on red edge excitation (REE), the spectral maximum falls nearly at the same frequency (at 480 nm) for all the concentration and coincides with the highest λ_{max} for the highest concentration obtained on SWE. This results in a decrease in the magnitude of EERS for the concentrated solutions. The fluorescence lifetime and the quantum yield also decrease with the concentration of the solutions. Thus in addition to the solvent relaxation process, the concentration quenching also takes place. Schafer and Rolling [37] have also observed concentration quenching of QSD fluorescence intensity and its decay however, they reported a mono-exponential exponential decay for QSD. Itoh and Azumi [38] have reported a decrease in concentration quenching on REE.

The decrease in lifetime, quantum yield, EERS and FWHM of emission band with increase in concentration along with the coincidence of λ_{max} at long time in TDFSS with the steady state fluorescence spectrum for the higher concentration suggest that at higher concentrations some additional dynamical process is competing with the solvent relaxation process.

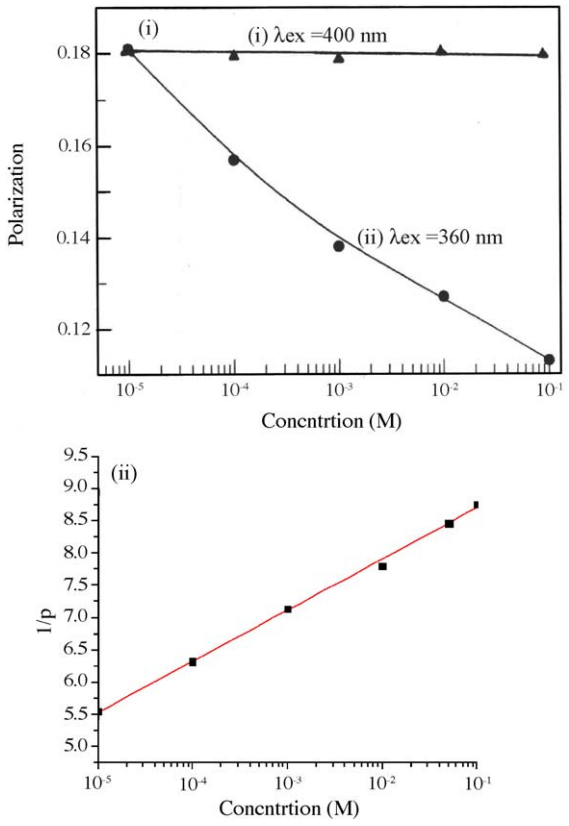

Fig. 6. Curve between (i) fluorescence polarization [P] vs. concentration [M] and (ii) $1/p$ (depolarization) vs. concentration of QSD in mole.

In a solution, the excited state of the molecular ensemble can be considered as a distribution of quasi continuum excited states. The emission from a higher state is overlapped with the absorption transition to a lower lying state, making conditions for excitation energy transfer favorable, particularly when the concentration is increased. The degradation of energy in this manner ultimately terminates into the emission from the lowest level of the system, which falls at 454 nm (SWE position) and 465 nm (REE position) for the highest concentration (10^{-2} M). Such an energy transfer, known as energy migration, results in a successive decrease in the lifetime with the increase in solute concentration, which follows the Stern–Volmer quenching kinetics. The occurrence and nature of the TDFSS as found above for higher concentration can be attributed to energy migration along with the solvent relaxation processes.

To verify that the energy migration is responsible for dependence of various observed parameters on concentration, the concentration depolarization experiments were carried out as shown in Fig. 6(i). It shows that fluorescence polarization decreases, i.e. depolarization increases, with increase in concentration. This clearly indicates that the migration of excitation energy among emitting molecules occurs as the concentration of the solute increases. The critical transfer distance (R_0) for energy migration has been calculated using

these concentration data and using the equation [39]:

$$\left(\frac{1}{p}-\frac{1}{3}\right)=\left(\frac{1}{p_0}-\frac{1}{3}\right)\left(1+\frac{4\pi NR_0^6C\times 10^3}{15(2a)^3}\right) \quad (6)$$

where p and p_0 is the final and initial polarization at highest (10^{-1} M) and lowest (10^{-5} M) concentration respectively, N the Avogadro number, C the concentration, and "a" is the radius (3.5 Å) of the molecular system. In Fig. 6(ii), we have plotted $1/p$ against concentration of QSD, which is in agreement with above equation. From the slop of the straight line in the figure, R_0 comes out to be 18.7 Å showing that for concentration depolarization is due to energy migration.

Again we calculated R_0 from Forester equation [40]:

$$R_{OD}=\sqrt[3]{\frac{3000}{4\pi^{3/2}NC_{OD}}} \quad (7)$$

where C_{OD} is the critical transfer concentration at which decay time become half of its initial value. Hear critical transfer concentration is 5×10^{-2} M as shown in Table 1. It comes out 20.0 Å. These values are quite in agreement with the depolarization measurements. This shows that concentration depolarization is due to energy migration among donor through Forester transfer mechanism of dipole–dipole interaction. Such concentration depolarization due to energy migration has been shown experimentally and theoretically by various workers [41,42].

The linear decrease in solvent relaxation time τ_r and EERS with concentration as shown in Fig. 7i and ii shows that solvent relaxation rate increases with increase in concentration. Further a linear increase of depolarization with concentration (Fig. 6ii) also indicates the increase of energy migration. Thus, at lower concentrations the solvent relaxation is higher than the migration whereas, at higher concentrations the energy migration becomes dominant. This is because on increasing concentration solute–solute interaction increases and solute solvent interaction decreases.

At higher concentration, on SWE the energy migration channel becomes important and subsequent quenching takes place. On REE, however, the solvent relaxation is dominant at low concentration giving rise to Stoke's Shifted emission with an EERS of 840 cm^{-1}, whereas at higher concentration the energy migration competes the solvent relaxation and thereby reduces the EERS so much so that for highest concentration used (10^{-2} M), EERS becomes 375 cm^{-1}. The fact that λ_{max} in TDFSS coincide with the steady state fluorescence maximum obtained for 10^{-2} M concentration but not for 10^{-5} M concentration, also suggests the dominance of energy migration at higher concentration. Similarly, both the decrease in FWHM of emission band and τ_r with increase in concentration, are attributable to dominating fast energy migration process relative to solvent relaxation at higher concentrations.

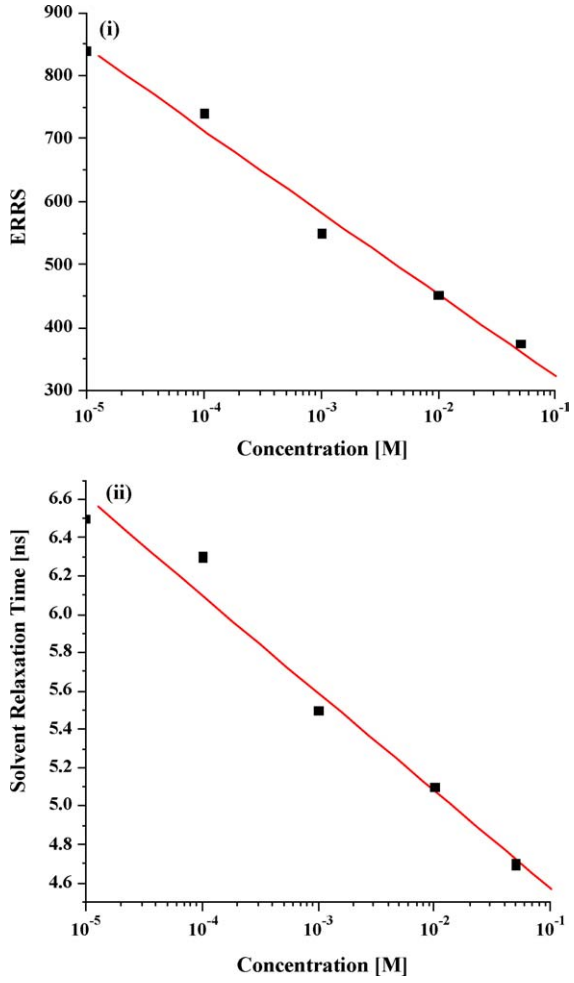

Fig. 7. Curve between (i) EERS vs. concentration and (ii) solvent relaxation time (τ_r) vs. concentration of QSD in mole.

4. Conclusions

We propose that on SWE, the concentration dependent red shift of emission maximum and a decrease in fluorescence lifetimes and quantum yield at higher concentrations of QSD is due to the singlet–singlet non-radiative energy transfer from molecular higher energy emitting state to those of lower energy emissions known as energy migration. On REE, the decrease of EERS with concentration is also attributed to energy migration. The occurrence and nature of TDFSS, the decrease in τ_r and not the least, the observed concentration depolarization supports such energy migration. The observed photo-physical behavior for the higher concentrations can be attributed to the energy migration process along with the solvent relaxation process.

Acknowledgments

Authors are thankful to Dr. A. Pradhan, Laser Raman Laboratory, IIT Kanpur, in helping us to carrying out the

depolarization measurements. One of the authors (HM) is thankful to CSIR (India) for Research Associate fellowship.

References

[1] W.H. Melhuish, J. Phys. Chem. 62 (1960) 762.
[2] D.W. Moss, Clin. Chim. Acta 5 (1960) 283.
[3] S.G. Schulman, R.M. Threatte, A.C. Capomacchia, W.L. Poul, J. Pharm. Sci. 63 (1974) 876.
[4] A. Gafni, R.P. Detoma, R.E. Manrow, L. Barnad, Biophys. J. 17 (1977) 155.
[5] V.I. Stenberg, E.F. Travecedo, J. Org. Chem. 35 (1970) 4131.
[6] H.C. Bϕrresen, Acta Chem. Scand. 19 (1965) 2089.
[7] R.F. Chen, Anal. Biochem. 19 (1967) 374.
[8] A.N. Fletcher, J. Phys. Chem. 72 (1968) 2742.
[9] A.P. Demchenko, Luminescence 17 (2002) 19.
[10] K. Itoh, T. Azumi, Chem. Phys. Lett. 22 (1973) 395.
[11] R. Schugler, I. Isenberg, Rev. Sci. Instrum. 42 (1971) 813.
[12] D.V. O'Connor, S.R. Meech, D. Phillips, Chem. Phys. Lett. 88 (1982) 22.
[13] D.A. Barrow, B.R. Lentz, Chem. Phys. Lett. 104 (1984) 161.
[14] S.R. Meech, D. Phillips, J. Photochem. 23 (1983) 193.
[15] P. Gangola, N.B. Joshi, D.D. Pant, Chem. Phys. Lett. 51 (1977) 144.
[16] D. Pant, U.C. Tripathi, G.C. Joshi, H.B. Tripathi, D.D. Pant, J. Photochem. Photobiol. A: Chem. 51 (1990) 313.
[17] S. Pant, H.B. Tripathi, D.D. Pant, J. Photochem. Photobiol. A: Chem. 85 (1995) 33.
[18] D. Pant, H.B. Tripathi, D.D. Pant, J. Lumin. 50 (1991) 249;
D. Pant, H.B. Tripathi, D.D. Pant, J. Lumin. 51 (1992) 223.
[19] H. Mishra, Ph.D. Thesis, Kumaun University, Nainital, 2002.
[20] D. Pant, H.B. Tripathi, D.D. Pant, J. Photochem. Photobiol. A: Chem. 56 (1991) 207.
[21] C.J. Rocha, M.H. Gehlen, R.D. Silva, P.M. Donate, J. Photochem. Photobiol. A: Chem. 123 (1999) 129.
[22] G.D. Geddes, Meas. Sci. Tech. 12 (2001) 53.
[23] M.A. Nava, M.O.B. Garcia, L.A.D. Torres, S.C. Cenda, T.A. Kong, Opt. Mater. 13 (1999) 327.
[24] H.C. Joshi, A. Upadhyay, H. Mishra, H.B. Tripathi, D.D. Pant, J. Photochem. Photobiol. A: Chem. 122 (1999) 185.
[25] H. Mishra, H.B. Tripathi, D.D. Pant, Rev. Sci. Instrum., in press.
[26] S. Hirayama, T. Inoue, Chem. Phys. Lett. 115 (1985) 79.
[27] S. Strickler, R.A. Berg, J. Chem. Phys. 37 (1962) 814.
[28] J.N. Damas, G.A. Crosby, J. Phys. Chem. 75 (1971) 991.
[29] N.G. Bakhshiev, Yu.T. Mazurenko, I.V. Piterskaya, Opt. Spectrosc. 21 (1966) 307.
[30] J.R. Lakowicz, Principles of Fluorescence Spectroscopy, Plenum Press, 1990.
[31] R. Jimenez, G.R. Fleming, P.V. Kumar, M. Maroncelli, Nature 369 (1994) 471.
[32] R.W. Impey, P.A. Madden, I.R. Mcdonald, J. Phys. Chem. 87 (1983) 5071.
[33] E. Guardia, J.A. Padro, J. Phys. Chem. 94 (1990) 6049.
[34] Y. Wang, Y. Tominaga, J. Chem. Phys. 101 (1994) 3453.
[35] S. Obst, H. Bradaczek, J. Phys. Chem. 100 (1996) 15677.
[36] A. Tongraar, K.R. Liedl, B.M. Rode, J. Phys. Chem. A 101 (1997) 6299.
[37] F.P. Schafer, K. Rolling, Z. Phys. Chem. 40 (1964) 198.
[38] K. Itoh, T. Azumi, J. Chem. Phys. 62 (1975) 343.
[39] C.A. Parker, Photoluminescence of Solutions, Elsevier Science Publishing Company, Amsterdam, 1968.
[40] Th. Förster, Discuss. Faraday Soc. 27 (1959) 7;
Th. Förster, Z. Naturforsch 49 (1949) 1321.
[41] C. Bojarski, J. Lumin. 9 (1974) 40.
[42] H.C. Joshi, H. Mishra, H.B. Tripathi, T.C. Pant, J. Lumin. 90 (2000) 17–25.